AMERICAN SOCIETY FOR MICROBIOLOGY | Journal of Virology®

VIRUS-CELL INTERACTIONS

The Amino Terminus of Herpes Simplex Virus 1 Glycoprotein K (gK) Is Required for gB Binding to Akt, Release of Intracellular Calcium, and Fusion of the Viral Envelope with Plasma Membranes

Farhana Musarrat,[a] Nithya Jambunathan,[a] Paul J. F. Rider,[a] V. N. Chouljenko,[a] K. G. Kousoulas[a]

[a]Division of Biotechnology and Molecular Medicine and Department of Pathobiological Sciences, School of Veterinary Medicine, Louisiana State University, Baton Rouge, Louisiana, USA

ABSTRACT Previously, we have shown that the amino terminus of glycoprotein K (gK) binds to the amino terminus of gB and that deletion of the amino-terminal 38 amino acids of gK prevents herpes simplex virus 1 (HSV-1) infection of mouse trigeminal ganglia after ocular infection and virus entry into neuronal axons. Recently, it has been shown that gB binds to Akt during virus entry and induces Akt phosphorylation and intracellular calcium release. Proximity ligation and two-way immunoprecipitation assays using monoclonal antibodies against gB and Akt-1 phosphorylated at S473 [Akt-1(S473)] confirmed that HSV-1(McKrae) gB interacted with Akt-1(S473) during virus entry into human neuroblastoma (SK-N-SH) cells and induced the release of intracellular calcium. In contrast, the gB specified by HSV-1(McKrae) gKΔ31-68, lacking the amino-terminal 38 amino acids of gK, failed to interact with Akt-1(S473) and induce intracellular calcium release. The Akt inhibitor miltefosine inhibited the entry of McKrae but not the gKΔ31-68 mutant into SK-N-SH cells. Importantly, the entry of the gKΔ31-68 mutant but not McKrae into SK-N-SH cells treated with the endocytosis inhibitors pitstop-2 and dynasore hydrate was significantly inhibited, indicating that McKrae gKΔ31-68 entered via endocytosis. These results suggest that the amino terminus of gK functions to regulate the fusion of the viral envelope with cellular plasma membranes.

IMPORTANCE HSV-1 glycoprotein B (gB) functions in the fusion of the viral envelope with cellular membranes during virus entry. Herein, we show that a deletion in the amino terminus of glycoprotein K (gK) inhibits gB binding to Akt-1(S473), the release of intracellular calcium, and virus entry via fusion of the viral envelope with cellular plasma membranes.

KEYWORDS Akt, fusion, HSV-1, calcium signaling, glycoprotein B (gB), glycoprotein K (gK)

Herpes simplex virus 1 (HSV-1) utilizes membrane fusion mediated by viral glycoproteins embedded within the viral envelope and expressed on infected cell surfaces to infect a variety of cell types and facilitate the spread of infectious virions to adjacent cells via virus-induced cell fusion, respectively (1).

HSV-1 entry mechanisms. Viral entry into cells can occur in a pH-independent manner via fusion of the viral envelope with cellular plasma membranes (PM), resulting in the deposition of viral capsids into the cytoplasm of infected cells. This mode of entry has been shown to be exclusively utilized during virus entry into neuronal axons (2–4). Also, a variety of other cell types, including African monkey kidney (Vero) cells, human

Received 24 October 2017 **Accepted** 17 December 2017

Accepted manuscript posted online 10 January 2018

Citation Musarrat F, Jambunathan N, Rider PJF, Chouljenko VN, Kousoulas KG. 2018. The amino terminus of herpes simplex virus 1 glycoprotein K (gK) is required for gB binding to Akt, release of intracellular calcium, and fusion of the viral envelope with plasma membranes. J Virol 92:e01842-17. https://doi.org/10.1128/JVI.01842-17.

Editor Richard M. Longnecker, Northwestern University

Address correspondence to K. G. Kousoulas, vtgusk@lsu.edu.

foreskin fibroblasts, HaCat cells, and rat kangaroo kidney (PtK2) cells, appear to be infected via direct fusion of the viral envelope with cellular plasma membranes (3, 5–8).

Alternatively, enveloped virions can enter a variety of cells by endocytosis into early endosomes, followed by pH-dependent and -independent fusion of the viral envelope with endosomal membranes, resulting in the release of virion capsids into the cytoplasm of infected cells (3, 9). HSV-1 prefers pH-dependent endocytosis for entering into CHO cells expressing nectin-1, HeLa cells, and human keratinocytes and pH-independent endocytosis in mouse melanoma (B78C10) cells (6, 10–14). The virus can spread from infected to uninfected cells by causing virus-induced cell fusion, allowing virions to enter into uninfected cells without being exposed to extracellular spaces.

Role of viral glycoproteins in virus entry. HSV-1 attaches to the cellular membrane by the attachment of viral glycoprotein B (gB) and gC to the glycosaminoglycan (GAG) moieties of cell surface proteoglycans (15, 16). Glycoprotein B can also interact with cellular receptors, including paired immunoglobulin-like type 2 receptor alpha (PILR), nonmuscle myosin heavy chain IIA (NMHC-IIA), and myelin-associated glycoprotein (MAG). Glycoprotein D binds to cellular receptors like herpesvirus entry mediator (HVEM; also called HveA), nectin-1 (HveC), and 3-O-sulfated heparan sulfate (17–23). Following binding of gD and gB, a conformational change that alters the conformation of gB occurs in gH/gL, triggering membrane fusion (24–29). Virus-induced cell fusion is thought to be mediated by a mechanism very similar to that occurring during fusion of the viral envelope with cellular membranes, inasmuch as viral glycoproteins gD, gB, gH, and gL and the presence of viral receptors are also required for virus-induced cell fusion (30–33). However, virus-induced cell fusion requires the presence of additional viral glycoproteins and membrane proteins, including gE, gI, gM, gK, and the UL20 and UL45 proteins (34–39).

Role of HSV-1 gK in membrane fusion. The UL20 and UL53 (glycoprotein K [gK]) genes are highly conserved in all alphaherpesviruses and encode proteins of 222 and 338 amino acids, respectively, each of which has four membrane-spanning domains (40–44). HSV-1 gK and UL20 interact functionally and physically, and these interactions are necessary for their coordinate intracellular transport, cell surface expression, and functions in virus-induced cell fusion, virus entry, virion envelopment, and egress from infected cells (37, 38, 43, 45–53). The gK/UL20 protein complex interacts with gB and gH and is required for gB-mediated cell fusion (39, 54). HSV-1 gK is a structural component of virions and functions in virion entry (50, 55, 56). Deletion of amino acids 31 to 68 within the amino terminus of gK (producing the gKΔ31-68 mutant) inhibits virus-induced cell-to-cell fusion and virus entry without drastically inhibiting virion envelopment and egress. We have shown that gK is essential for neuronal infection and virulence (57, 58). In addition, we have recently shown that HSV-1(McKrae) gKΔ31-68, specifying gK with a deletion of amino acids 31 to 68, was unable to efficiently infect mouse trigeminal ganglia after ocular infection of scarified mouse eyes (59). These results indicate that the amino terminus of gK plays a pivotal role in corneal infection and neuroinvasiveness (58, 59).

Role of cell signaling in membrane fusion. Akt is a serine/threonine kinase involved in important cellular signaling pathways (60). There are three isoforms of Akt: Akt-1, Akt-2, and Akt-3 (61–66). Although these isoforms are encoded by different genes, they share an N-terminal pleckstrin homology domain, a kinase domain, and a C-terminal regulatory domain (65). In this work, we focus on Akt-1, because it is the predominant isoform of Akt expressed ubiquitously, while Akt-2 and Akt-3 expression is limited to insulin-responsive tissues and brain or testes, respectively (67). Signaling through plasma membrane-embedded receptors activates the phosphoinositide 3-kinase (PI3K) signaling pathway, causing recruitment of Akt-1 to plasma membranes, where it is activated via phosphorylation at S473 and T308 (68–73). Herpesviruses express several proteins that alter the PI3K/Akt signaling pathway, which regulates cell survival, growth, apoptosis, inflammation, cell motility, calcium signaling, etc. (74). These regulatory

mechanisms can influence viral entry, replication, latency, and reactivation of HSV-1 (75, 76). Recently, it was shown that herpesvirus glycoprotein B activates Akt by phosphorylation and that gB physically interacts with Akt during virus entry (77). Herpesvirus infection also induces an intracellular calcium response (78). Binding of glycoprotein H (gH) of equine herpesviruses (EHV) to cellular integrin ($\alpha4\beta1$) triggers intracellular calcium signaling and phosphatidylserine (PS) exposure on the plasma membrane to facilitate EHV-1 entry (79). Furthermore, Akt silencing or the Akt inhibitor miltefosine inhibited calcium signaling and virus entry into cells (77).

In this report, we show that gK is required for entry via fusion of the viral envelope with cellular membranes. The underlying mechanism involves a role for gK in the regulation of intracellular calcium release, and expression of the version of Akt-1 phosphorylated at serine residue 473 [Akt-1(S473)] on cell surfaces is required for binding to gB during virus entry.

RESULTS

The gKΔ31-68 mutation causes decreased sensitivity to miltefosine-mediated inhibition of virus entry. Previous work has shown that the Akt inhibitor miltefosine prevents HSV entry into cells (77). Miltefosine mimics the PH domain of Akt and blocks the recruitment of Akt to the inner leaflet of the plasma membrane (80). To confirm these findings, we tested whether Akt is important for HSV-1 entry using miltefosine. Nearly confluent monolayers of Vero cells were pretreated for 15 min with increasing doses of miltefosine, and virus entry experiments were performed as described in Materials and Methods. Miltefosine at concentrations of 200 μM and higher was toxic to Vero cells, while up to 100 μM the drug was well tolerated. As expected, the McKrae wild-type (WT) strain was inhibited in a dose-dependent manner, with more than 90% inhibition being achieved at 100 μM miltefosine. Surprisingly, gKΔ31-68 mutant entry was not inhibited (Fig. 1A). The effect of miltefosine on virus entry was also tested in SK-N-SH cells using the proximity ligation assay (PLA) for virus entry (see Materials and Methods). Single plaque assays reflecting each incoming virus cannot be performed on SK-N-SH cells, since they do not allow easily visible plaque formation. A miltefosine concentration of 50 μM and higher was toxic to the SK-N-SH cells, while at concentrations of up to 30 μM there were no apparent toxic effects observed. Briefly, PLA reveals the deposition of capsids into the cytoplasm of infected cells by detecting the interaction of the HSV-1 UL37 protein with dynein, while cell surface-bound virions are detected via the interaction of gD with nectin-1 (81). Both viruses attached to cell surfaces equally well; however, at the maximum concentration of miltefosine tested (30 μM, since 100 μM miltefosine was toxic to SK-N-SH cells), McKrae wild-type virus entry was drastically inhibited, while gKΔ31-68 virus entry was unaffected (Fig. 1B).

The gKΔ31-68 mutation inhibits gB binding to Akt-1(S473). Previous work has shown that gB binds to Akt and Akt is required for virus entry (77). The ability of HSV-1 gB to bind the Akt-1(S473) specified by the gKΔ31-68 mutant virus was tested using the proximity ligation assay (PLA) and a two-way coimmunoprecipitation assay. We focused on the detection of Akt-1(S473) due to the availability of highly reactive Akt-1(S473) antibody (see Materials and Methods). PLA using specific antibodies against Akt-1(S473) and gB detected a close association of gB and Akt-1(S473) in McKrae-infected but not in McKrae gKΔ31-68-infected SK-N-SH cells at 1 h postinfection (hpi) at a multiplicity of infection (MOI) of 10 (Fig. 2A).

To support the results from the PLA, two-way coimmunoprecipitation assays were performed using anti-gB and anti-Akt-1 monoclonal antibodies, and the presence of gB and Akt-1 in immunoblots of infected SK-N-SH cell lysates and in immunoprecipitates was detected with either anti-gB or anti-Akt-1 antibody. Similar amounts of gB were detected in either McKrae- or gKΔ31-68 mutant-infected lysates, with gB appearing as a two major protein species migrating with apparent molecular masses of 130 and 120 kDa, most likely representing the high-mannose precursor and the fully glycosylated species, respectively, as we have reported previously (54, 81, 82). Similar amounts of Akt-1(S473) were detected in both McKrae- and gKΔ31-68 mutant-infected SK-N-SH cell

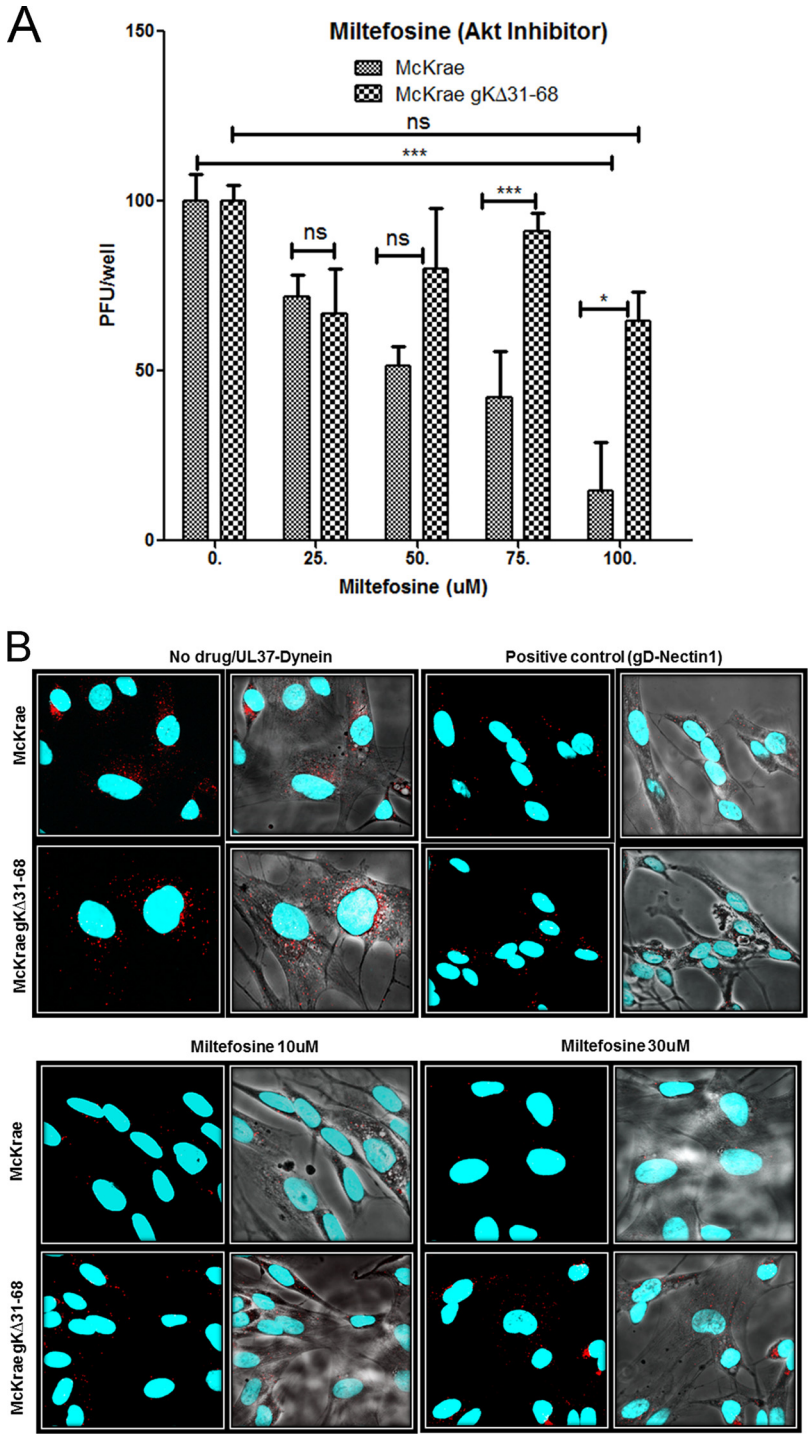

FIG 1 Effect of an Akt inhibitor on HSV-1 entry. (A) Vero cells were treated with a series of dilutions of the Akt inhibitor miltefosine (labeled Akt inhibitor) for 15 min and then adsorbed with McKrae and McKrae gKΔ31-68 (100 PFU) for 1 h at 4°C. After incubation at 37°C for 48 h, the plaques (the number of PFU) were counted using crystal violet staining. *, $P < 0.05$ between McKrae and gKΔ31-68 viruses; ***, $P < 0.001$ versus no-drug-treated control; ns, no significance versus no-drug-treated control. Statistical comparison was conducted by GraphPad Prism software using ANOVA with a *post hoc t* test with the Bonferroni adjustment. Bars represent 95% confidence intervals about the means. (B) SK-N-SH cells were treated with miltefosine for 15 min and infected with McKrae or McKrae gKΔ31-68 (MOI = 10) for 1 h at 37°C, and the proximity ligation assay (PLA) was performed. Confocal microscopy was used to detect bright red spots, which indicate an interaction between two proteins after drug treatment, at a magnification of ×63 with oil immersion. The interaction between UL37 (capsid protein) and dynein (cellular protein) was used as a measure of entry of the virus. The interaction between gD and nectin-1 was used as a positive PLA control in this experiment. DAPI was used to stain the nuclei of the cells.

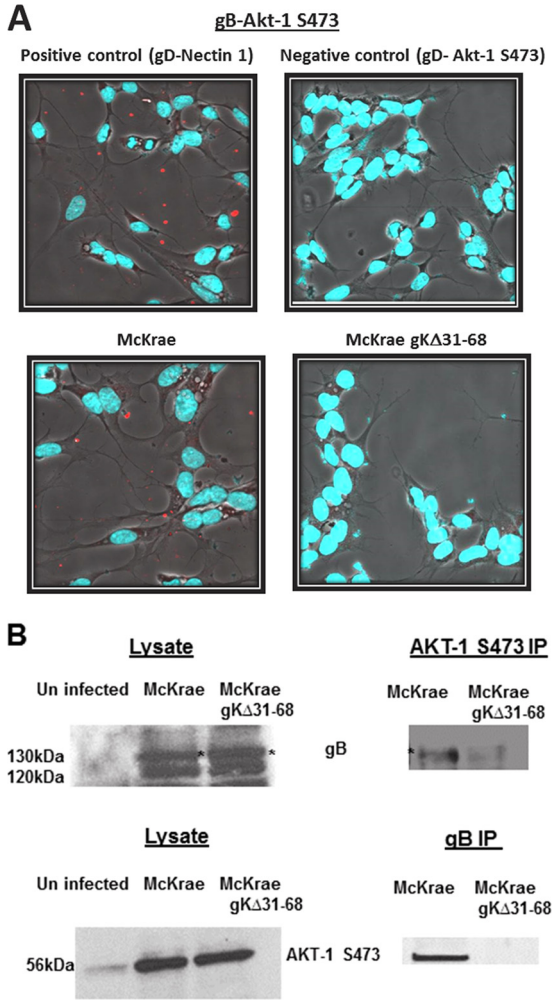

FIG 2 Interaction between gB and Akt-1(S473). (A) Proximity ligation assay showing the interaction between gB and Akt-1(S473) in McKrae- and McKrae gKΔ31-68-infected SK-N-SH cells at 1 h postinfection at an MOI of 10. The gD–nectin-1 interaction was used as a positive control, and the gD–Akt-1(S473) interaction was used as a negative control. Confocal microscopy was used to detect the bright red spots that suggest the interaction between two proteins. DAPI was used to stain the nuclei of the cells. Magnifications, ×63 with oil immersion. (B) Two-way immunoprecipitation (IP) showing the gB–Akt-1(S473) interaction in McKrae and McKrae gKΔ31-68 virus-infected (MOI = 10) SK-N-SH cell lysates.

lysates; however, the overall levels of Akt-1(S473) were substantially higher in infected cells than in uninfected cells, indicating that both viruses induced Akt-1 phosphorylation equally well. Anti-gB antibody detected the presence of gB in anti-Akt-1(S473) immunoprecipitates of McKrae-infected SK-N-SH cellular lysates at 1 hpi; however, a substantially smaller amount of gB was detected in the immunoprecipitate from gKΔ31-68 mutant-infected cellular lysates. Similarly, the anti-Akt-1 antibody detected Akt-1 in anti-gB immunoprecipitates of McKrae- but not gKΔ31-68 mutant-infected SK-N-SH cell lysates (Fig. 2B).

The gKΔ31-68 mutation fails to induce the release of intracellular calcium. Intracellular free calcium regulates a variety of cellular processes, including sperm-egg fusion, contraction, secretion, cell growth, and apoptosis (83). Previous work indicated that HSV-1 infection triggers the release of intracellular calcium, which is required for virus entry (77, 84). Inhibition of Akt prevents calcium release and HSV-1 entry (77). To test whether the McKrae and gKΔ31-68 viruses triggered intracellular calcium release, we utilized the calcium indicator Fura-2-acetoxymethyl ester (Fura-2AM), which binds free calcium in the cytosol immediately following infection with gradient-purified virions. The relative amount of calcium was calculated every minute over the 1-h time

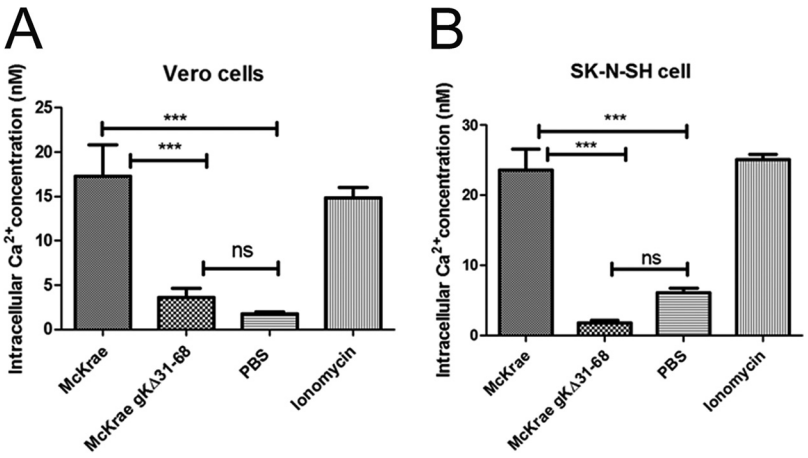

FIG 3 HSV-1 triggers intracellular calcium release. Vero cells (A) and SK-N-SH cells (B) were grown in a 96-well black clear-bottom plate and treated with Fura-2AM (25 μM) for 30 min at 37°C. After washing, the cells were adsorbed with purified McKrae and McKrae gKΔ31-68 (both at an MOI of 10) at 4°C for 1 h and then shifted to 37°C to measure the absorbance every minute over an hour. The ratio of bound to unbound dye (340/380 nm) was measured, the intracellular calcium concentration was calculated, and the average values are presented. Ionomycin was used as a positive control, and 1× PBS was used as a negative control. ***, $P < 0.001$ versus the PBS control; ns, no significance versus the PBS control. Statistical comparison was conducted by GraphPad Prism software using ANOVA with a *post hoc t* test with the Bonferroni adjustment. Bars represent the 95% confidence intervals about the means.

period of virus entry at 37°C, and the average values are presented (see Materials and Methods). The McKrae wild-type virus triggered almost 14 and 20 times higher levels of calcium release than the gKΔ31-68 mutant virus in Vero and SK-N-SH cells, respectively (Fig. 3A and B).

The gKΔ31-68 mutation fails to cause PS and Akt-1(S473) expression on infected Vero cell surfaces. Intracellular calcium activates flippase (scramblase) enzymes, which function in flipping the inner leaflet to the outer leaflet of the plasma membrane (PM). Phosphatidylserine (PS) resides on the inner leaflet of the PM (85). Therefore, the presence of PS on cell surfaces is indicative of membrane flipping (85). Although Akt is a cytosolic protein, Akt is recruited to the inner leaflet of the membrane by phosphatidylinositol (3,4,5) triphosphate (PIP3)/PH domain binding. The PH domain of Akt is responsible for the anchoring (80). Previous work suggested that equine herpesvirus 1 (EHV-1) infection of epithelial cells triggers exposure of PS from the inner leaflet of the plasma membrane to the outer surface (79). We investigated whether HSV-1 infection causes expression of PS on infected Vero cell surfaces. Vero cells were adsorbed with both McKrae and gKΔ31-68 viruses at 4°C for 1 h, and then infected cell cultures were shifted to 37°C for 5 min. Fluorescein isothiocyanate (FITC)-conjugated annexin V staining of PS showed that McKrae wild-type virus infection caused expression of PS on cell surfaces (Fig. 4A). Specifically, there was at least a 3-fold higher level of PS expression in McKrae-infected cells than gKΔ31-68 mutant-infected cells, as revealed by quantitative analysis of the fluorescent signals (Fig. 4B).

Both the McKrae and gKΔ31-68 viruses caused phosphorylation of Akt-1 at S473 (Fig. 2B), indicating that Akt-1 was efficiently associated with the inner leaflet of the plasma membrane, since Akt-1 phosphorylation occurs after Akt-1 is bound to plasma membranes (80). The previous results obtained with PS indicated that the gKΔ31-68 mutant failed to flip inner leaflet lipids to the outer membrane leaflet. We tested whether the inability of the gKΔ31-68 mutant to flip PS from the inner to the outer membrane leaflet was also true for Akt-1. Vero cells were infected with either McKrae VP26-enhanced green fluorescent protein (EGFP) or gKΔ31-68 mutant VP26-EGFP at 37°C for 30 min. To detect the cell surface expression of Akt-1, infected Vero cells were reacted with rabbit anti-Akt-1 antibody under live conditions for 30 min at 37°C. Subsequently, the cells were washed, fixed with formalin, and reacted with goat anti-rabbit immunoglobulin

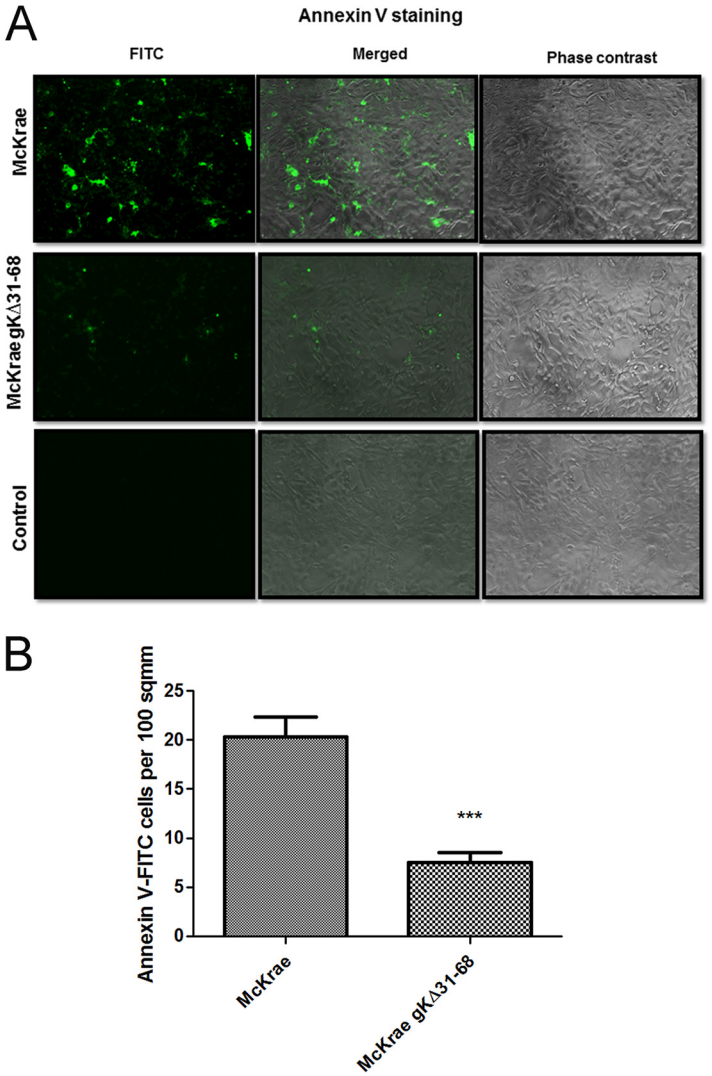

FIG 4 Phosphatidylserine exposure on cell surface. (A) Vero cells were adsorbed with either McKrae or McKrae gKΔ31-68 at an MOI of 10 for 1 h at 4°C, and then the 8-well chamber slides were shifted to 37°C for 5 min. Cells were live stained with FITC-conjugated annexin V to detect phosphatidylserine on the surface. Fluorescent (FITC), phase-contrast, and merged images of the infected and uninfected control Vero cells are presented. A fluorescence microscope was used to take the images. Magnifications, ×40. (B) The number of cells labeled by FITC-conjugated annexin V per area of 100 mm^2 was counted. Values were normalized to those for the uninfected control wells. Statistical comparison was conducted by GraphPad Prism software using Student's *t* test. Bars represent the 95% confidence intervals about the means. A comparison was made between the viruses.

antibody conjugated to Alexa Fluor 594. To validate the experimental conditions used to detect cell surface-expressed Akt-1, antidynein antibody was reacted with Vero cells under live conditions for 30 min at 37°C, immediately followed by formalin fixation. As expected, the antidynein antibody failed to react with dynein under these conditions, indicating that the antidynein antibody did not enter into cells during the 30-min incubation at 37°C. In contrast, the antidynein antibody reacted efficiently with dynein when the cells were fixed and permeabilized with methanol. The emission of fluorescence by viral VP26-EGFP was used to detect the presence of virions. Whole-cell Akt-1 expression was similarly detected with anti-Akt-1 antibody after cellular permeabilization and fixation with methanol (Fig. 5A to C) (see Materials and Methods). These experiments revealed that the gKΔ31-68 mutant failed to translocate Akt-1 to infected cell surfaces.

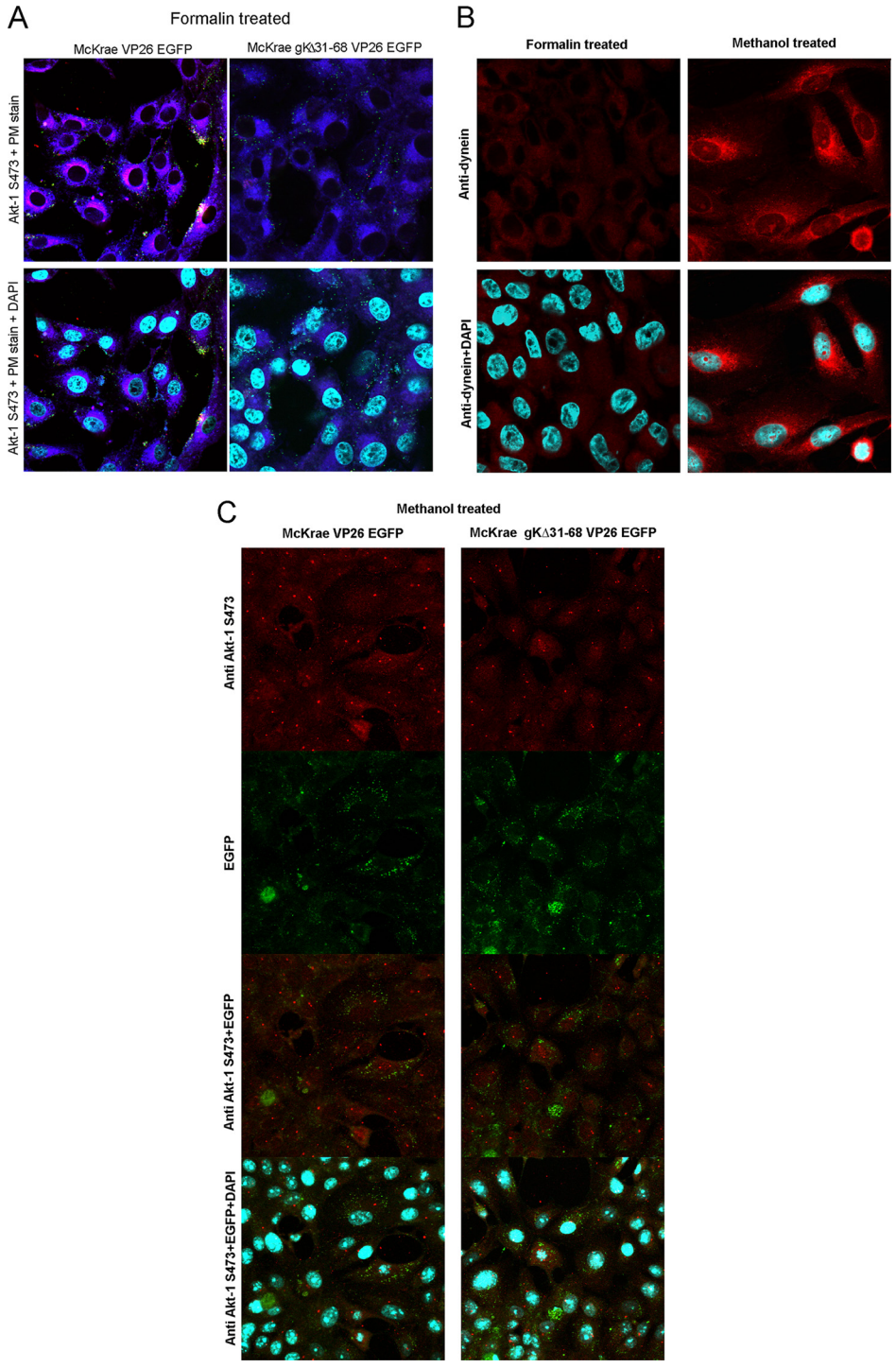

FIG 5 Akt-1(S473) exposure on the cell surface. (A) Vero cells were infected with either McKrae VP26-EGFP or McKrae gKΔ31-68 VP26-EGFP at an MOI of 10 for 30 min at 37°C and were then reacted with rabbit anti-Akt-1(S473) antibody (1:100) under live conditions for 30 min at 37°C. After acid washing, the cells were formalin fixed and stained with anti-rabbit immunoglobulin antibody conjugated with Alexa Fluor 594 (red) and plasma membrane stain (purple). The slides were mounted with mounting medium with DAPI (cyan). (B) (Top) Vero cells were either reacted with mouse antidynein antibody and formalin fixed (left) or fixed and permeabilized with methanol and reacted with mouse antidynein antibody for 30 min at 37°C (right). (Bottom) Cells were washed with PBS and stained with anti-mouse immunoglobulin antibody conjugated with Alexa Fluor 594 (red) and were mounted with mounting medium with DAPI. (C) Vero cells were infected with either McKrae VP26-EGFP or McKrae gKΔ31-68 VP26-EGFP for an hour at 37°C and then fixed and permeabilized with methanol. After washing, the cells were reacted with rabbit anti-Akt-1(S473) antibody for 30 min at 37°C and stained with anti-rabbit immunoglobulin antibody conjugated with Alexa Fluor 594 (red). The slides were mounted with mounting medium with DAPI. Confocal microscopy was used to take the images. Magnifications, ×63 with oil immersion.

The gKΔ31-68 mutation forces virus entry via endocytosis. Recently, it was shown that a lack of intracellular calcium release and scramblase activity caused EHV-1 to enter into cells via endocytosis instead of fusion of the viral envelope with cellular plasma membranes (79). Therefore, we tested the ability of the endocytosis inhibitors pitstop-2 and dynasore hydrate (79, 86, 87) to inhibit McKrae and gKΔ31-68 virus entry into SK-N-SH and Vero cells. Pitstop-2 and dynasore hydrate were used at concentrations of up to 50 and 80 μM, respectively, for Vero cells, since higher concentrations (75 and 100 μM, respectively) were toxic for Vero cells. For SK-N-SH cells, the corresponding nontoxic concentrations used were 30 μM (pitstop-2) and 80 μM (dynasore hydrate), since concentrations higher than 50 μM (pitstop-2) and 100 μM (dynasore hydrate) were toxic to SH-N-SH cells.

Pitstop-2 blocks clathrin, which coats the endocytic vesicle, and dynasore hydrate is an inhibitor of dynamin, which creates a nick to release the endosome to the cytoplasm (86, 87). SK-N-SH cells were treated with both drugs for 15 min at 37°C and then infected with either McKrae or gKΔ31-68 viruses. An MOI of 10 was used for SK-N-SH cells. Virus entry was detected using PLA following 1 h of infection in the case of SK-N-SH cells, as described previously (81), Briefly, PLA detects the deposition of capsids into the cytoplasm of infected cells by detecting the interaction of the HSV-1 UL37 protein with dynein, while cell surface-bound virions are detected via the interaction of gD with nectin-1 (81). Similar numbers of McKrae and gKΔ31-68 virions were attached to SK-N-SH cells, as detected by PLA (Fig. 6A). Treatment of cells with either pitstop-2 (30 μM) or dynasore hydrate (80 μM) reduced the number of virions detected within the cytoplasm of SK-N-SH cells, while the combined use of both inhibitors (pitstop-2 at 30 μM plus dynasore hydrate at 80 μM) substantially reduced the number of gKΔ31-68 virus capsids detected within SK-N-SH cells but not McKrae-infected SK-N-SH cells (Fig. 6A). Similarly, when Vero cells were treated with the same drugs and infected with both the McKrae and gKΔ31-68 viruses for 48 h at 37°C at 100 PFU, a dose-dependent reduction in the number of plaques was observed in the case of the gKΔ31-68 mutant but not in the case of the McKrae wild-type virus (Fig. 6B).

DISCUSSION

HSV-1 has been shown to enter into neuronal axons exclusively via fusion of the viral envelope with the synaptic axonal membrane, mediated by viral glycoprotein B (gB). This fusion event leads to the deposition of virion capsids that are subsequently transported in a retrograde manner to the neuronal cell bodies (2). However, HSV-1 can enter into different cells via either fusion of the viral envelope with cellular plasma membranes or endocytosis of the enveloped particle into early endosomes, where they can be released presumably via fusion of the viral envelope with endosomal membranes. This fusion event is facilitated by the low-pH environment within endosomes that triggers gB-mediated fusion. We have recently shown that the amino terminus of HSV-1 glycoprotein K (gK) interacts with gB and regulates gB-mediated entry into neuronal axons and subsequent infection of ganglionic neurons, required for establishment of latency (39). Herein, we show for the first time that virions unable to enter into neuronal axons can enter into Vero cells and SK-N-SH neuronal cells via endocytosis. Moreover, we show that binding of gB to Akt-1 phosphorylated at S473 on the plasma membrane is associated with the ability of the virus to enter via fusion at the plasma membrane. These results identify gK to be a regulator of entry via fusion of the viral envelope with cellular plasma membranes.

HSV-1 gK is required for Akt binding, intracellular calcium release, phosphatidylserine and Akt translocation to the outer plasma membrane leaflet, and fusion of the viral envelope with cellular plasma membranes. The mechanism by which gB mediates membrane fusion during virus entry, as well as in cell-to-cell fusion, remains enigmatic. The prevalent hypothesis is that the initial binding of gD to the cellular receptor nectin-1 or HVEM triggers a conformational change in gH/gL that ultimately triggers gB's fusogenicity (28). Conventional fusion models call for the juxtaposition of hydrophobic segments of the fusion protein within the apposed

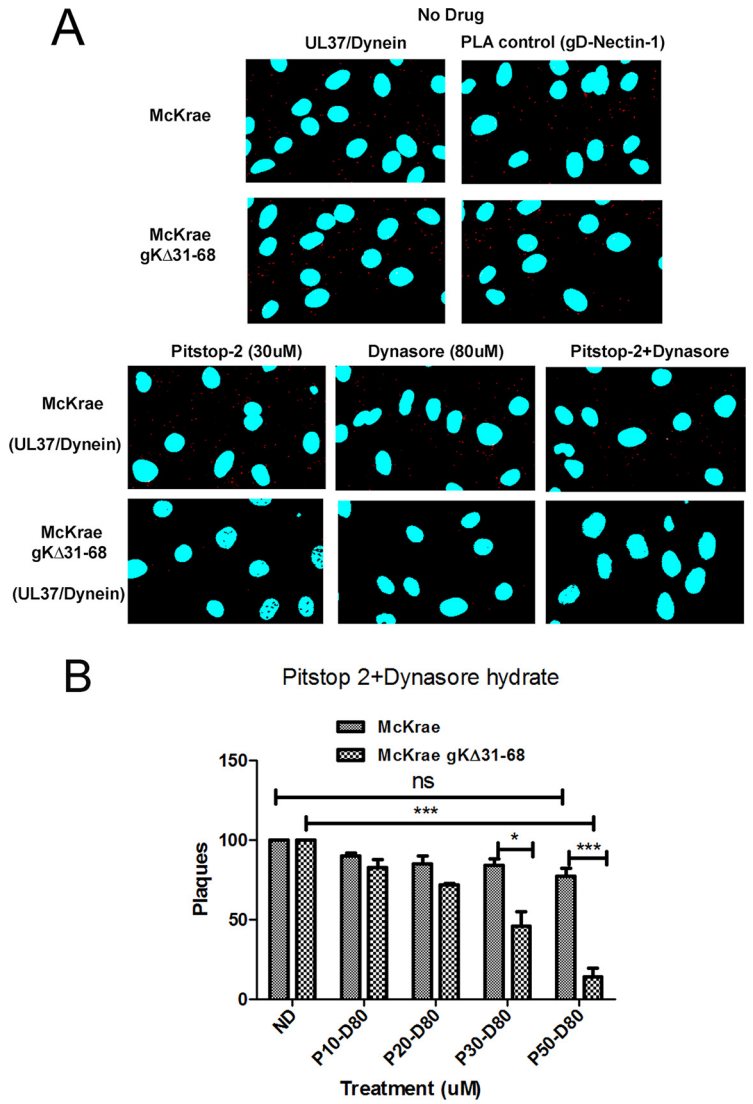

FIG 6 Endocytosis assay. (A) SK-N-SH cells were treated with no drug, 30 μM pitstop-2, or 80 μM dynasore hydrate or with 30 μM pitstop-2 plus 80 μM dynasore hydrate in combination for 30 min at 37°C. Cells were infected with either McKrae or McKrae gKΔ31-68 for 1 h at an MOI of 10 at 37°C and then prepared for PLA. The UL37-dynein interaction was used as a measure of entry of the viral capsid into the cell, and the gD–nectin-1 interaction was used as a PLA control. Confocal microscopy was used to detect the bright red spots that suggest the interaction between two proteins. DAPI was used to stain the nuclei of the cells. Magnifications 63× with oil immersion. (B) Vero cells were treated with combined doses of pitstop-2 at 10, 20, 30, or 50 μM (P10, P20, P30 and P50, respectively) and dynasore hydrate at 80 μM (D80) for 30 min at 37°C and then infected with 100 PFU the McKrae or McKrae gKΔ31-68 virus for 1 h at 37°C (without washing the drug off). After infection, the wells were washed with PBS and methylcellulose was added. The plaques (the numbers of PFU) were counted using crystal violet staining after 48 h. *, $P < 0.05$ versus the no-drug-treated control (ND); ***, $P < 0.001$ versus the no-drug-treated control. Statistical comparison was conducted by GraphPad Prism software using ANOVA with a *post hoc t* test with the Bonferroni adjustment. Bars represent the 95% confidence intervals about the means.

membrane, which leads to the creation of a membrane pore, which subsequently expands and merges the apposed membranes (29). Previous work by the Herold laboratory showed that gB can bind to Akt-1 phosphorylated at S473 during virus entry (77). Furthermore, phosphorylated Akt was hypothesized to be flipped to the outside membrane leaflet by scramblase, which can flip the inner membrane leaflet to the outer surface. The observed inability of the gKΔ31-68 virus to induce PS and Akt-1 translocation to the outer plasma membrane leaflets suggests that scramblase may not be activated. Presumably, scramblase is triggered via intracellular calcium release (84).

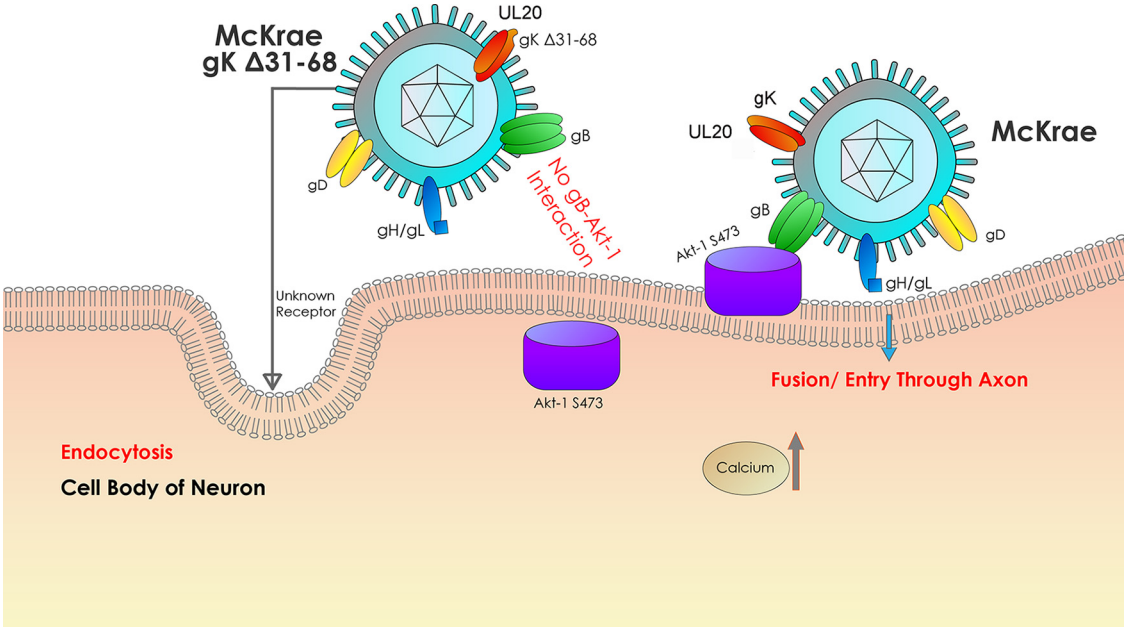

FIG 7 Model of HSV-1 entry into host cells. The schematic shows the molecules involved in HSV-1 entry via either endocytosis or fusion between the viral envelope and the cellular plasma membrane as well as the intracellular signaling that may be involved with these two entry pathways.

Previously, we have shown that gK binds to the amino terminus of gB and gH (54). Furthermore, previous results with EHV-1 have indicated that gH/gL binding to integrin αV is responsible for intracellular calcium release (79). Therefore, it is conceivable that destabilization of the gB/gH/gL/gK fusion complex may inhibit the triggering of calcium release by gH/gL. It is also possible that the lack of the amino terminus of gK alters the ability of gB to bind Akt-1(S473) in plasma membranes, since the amino terminus of gK binds to the amino terminus of gB. Alternatively, the amino terminus of gK may also bind cell surface-expressed integrins, causing intracellular calcium release. Additional experimentation is needed to clarify the role of gK and other viral glycoproteins in intracellular calcium release through engagement of cellular receptors.

It is widely accepted that HSV-1 enters into a variety of cells either by endocytosis of enveloped capsids or by fusion of the viral envelope with cellular membranes, or by both methods. We show here that endocytosis of enveloped virions utilizes a clathrin-mediated mechanism, while the fusion of viral envelopes with cellular plasma membranes is associated with binding to phosphorylated Akt and intracellular calcium release (Fig. 7). It is apparent that the inability of the gKΔ31-68 mutant to induce intracellular calcium release leads to inhibition of Akt-1 translocation from the inner leaflet to the outer leaflet of plasma membranes, resulting in the observed lack of interaction with gB.

HSV-1 gK's role has remained controversial over the years largely due to the fact that gK mutant viruses can enter into cells and replicate, albeit at highly reduced efficiencies (39). However, there is a plethora of evidence that gK and its interacting protein, UL20, play important roles in membrane fusion, exemplified by the fact that the gK gene is the locus of multiple mutations (40, 88–90) that cause extensive virus-induced cell fusion and that gK has been shown in our laboratory to be required for virus entry into neuronal axons (59). The fact that gK and UL20 are highly conserved among all alphaherpesviruses that have the predilection of infecting neurons via their axonal termini suggests that gK plays a crucial role in gB-mediated fusion events.

We have hypothesized and herein provide evidence that gK functions in mediating fusion between the viral envelope and cellular membranes, as well as in cell-to-cell fusion. gKΔ31-68 and gK-null viruses can enter into other than neuronal axonal

compartments via endocytosis, where the low pH of endosomes can trigger fusion of the viral envelope with endosomal membranes, releasing the virion into the cytoplasm without the need for the regulation provided by the presence of gK. HSV-1 entry into neuronal axons via fusion of the viral envelope with synaptic axonal membranes appears to be a highly regulated process in which gK plays a crucial role. An obvious explanation is that this exquisite mechanism of highly regulated virus entry is important not only for ensuring the successful entry of virions into the axoplasm of neurons but also for inducing the downstream signaling events that ensure the successful movement of virions in a retrograde manner and preparation of the neuronal cell as an optimum host for the establishment of viral latency.

Virus-cell fusion is known to trigger innate antiviral immune responses. Specifically, it has been reported that virus-cell fusion stimulated a type I interferon (IFN) response characterized by expression of IFN-stimulated genes (ISGs), engagement of Toll-like receptor 7 and 9 signaling, and *in vivo* recruitment of leukocytes (91). Apparently, intracellular calcium is induced during virus-cell fusion, as well as by fusogenic liposomes. Inhibition of calcium signaling abrogated IFN responses to HSV-1 entry (92, 93). These results suggest that virus-cell fusion and subsequent calcium signaling cause an innate immune response substantially different from that induced by virus entry via endocytosis. We have recently shown that intracellular vaccination of mice with the HSV-1(VC2) attenuated virus that contains the gKΔ31-68 mutation elicits strong humoral and cellular immune responses that protect mice against both HSV-1 and HSV-2 lethal, intravaginal challenge (94, 95), as well as ocular challenge with the human ocular clinical strain HSV-1(McKrae) (S. Naidu and K. G. Kousoulas, unpublished data). It is unclear at this point whether endocytotic entry abrogates the IFN response attributed to virus-cell fusion and the mechanism(s) by which this entry pathway leads to enhanced anti-HSV humoral and cellular immune responses. These topics are subject to ongoing investigations.

MATERIALS AND METHODS

Cell lines and viruses. African green monkey kidney (Vero) cells and cells of the SK-N-SH (HTB11) neuroblastoma cell line were obtained from the American Type Culture Collection (Manassas, VA) and were maintained in either Dulbecco's modified Eagle's medium or essential modified Eagle's medium (Gibco-BRL, Grand Island, NY) supplemented with 10% fetal calf serum and antibiotics, respectively. HSV-1 strain McKrae and McKrae gKΔ31-68 viruses were mostly used in this study. For some experiments, McKrae virus VP26-EGFP and McKrae gKΔ31-68 virus VP26-EGFP were used. McKrae gKΔ31-68 was engineered in our lab to express gK lacking the 38 amino acids immediately after the gK signal sequence and was cloned as a bacterial artificial chromosome, as described previously (59). McKrae virus VP26-EGFP and McKrae gKΔ31-68 virus VP26-EGFP were also constructed in our lab.

Reagents and antibodies. The primary antibodies used were as follows: mouse anti-gB antibody (Abcam), mouse anti-gD antibody (Abcam), rabbit anti-Akt-1(S473) antibody (Abcam), rabbit anti-nectin-1 antibody (Santa Cruz), rabbit anti-UL37 antibody (a gift from Frank J. Jenkins, University of Pittsburgh Cancer Institute), and mouse antidynein antibody (Abcam). Pitstop-2 was obtained from Abcam. Fura-2AM (catalog number AS-84015) was obtained from Anaspec. Miltefosine (catalog number sc-203135) was obtained from Santa Cruz Biotechnology, and dynasore hydrate was obtained from Sigma. An annexin V-FITC fluorescence microscopy kit was obtained from BD Bioscience. A Duolink *in situ* red starter kit mouse/rabbit was obtained from Sigma. Cell mask deep red plasma membrane stain was obtained from Thermo Fisher, and goat anti-rabbit immunoglobulin antibody conjugated with Alexa Fluor 594 was used as a secondary antibody.

Virus purification. Both the McKrae (WT) and the McKrae gKΔ31-68 viruses were purified as we have described earlier (96). Briefly, supernatants and cells from 6 T-150 flasks of Vero cells infected with the McKrae (WT) and McKrae gKΔ31-68 viruses were collected at 36 h postinfection (hpi) and purified twice by the use of 50 to 20% discontinuous iodixanol gradients, followed by a 20% iodixanol cushion. The resulting pellet was resuspended in 250 μl of phosphate-buffered saline (PBS) and used for the calcium assay.

Drug assay. Vero cells were treated with drugs for 15 min at 37°C, and then the viruses (100 PFU) were adsorbed at 4°C for an hour. Unbound viruses and unabsorbed drug were washed with PBS, and fresh media with methylcellulose were added onto the cells. The plates were incubated at 37°C for 48 h, and plaques were counted after being fixed with formalin and stained with crystal violet. In the case of SK-N-SH cells, drug treatment was done for 15 min, infection was done at an MOI of 10, and at 1 h postinfection the 8-well chamber slides were prepared for the respective PLA. Images were taken under a confocal microscope at a ×63 magnification with oil immersion.

Proximity ligation assay (PLA). SK-N-SH cells were grown on 8-well chamber slides (Nunc Lab-Tek II chamber slide system) and infected with the McKrae wild-type and McKrae gKΔ31-68 viruses at an MOI

of 10. At 1 h postinfection, the cells were fixed and permeabilized with ice-cold methanol for 10 min at −20°C. After three washes with PBS, the samples were blocked for 2 h at 37°C with Duolink blocking buffer in a humidity chamber. Primary antibodies that were raised in two different species were diluted in antibody diluting buffer and added to the samples, and the samples were incubated overnight at 4°C.

Mouse anti-gD antibody (Abcam) and rabbit anti-nectin-1 antibody (Santa Cruz) were used for gD and nectin-1 (positive control) detection, respectively. Mouse anti-gB (Abcam) and rabbit anti-Akt-1(S473) (Abcam) antibodies were used for HSV-1 McKrae wild type- and McKrae gKΔ31-68-infected cells to detect the gB–Akt-1(S473) interaction. Mouse antidynein antibody against intermediate chain I (Abcam) and rabbit anti-UL37 antibody (a gift from Frank J. Jenkins, University of Pittsburgh Cancer Institute) were used for dynein/UL37 detection as a measure of entry in the endocytosis assay.

Unbound primary antibodies were removed by washing with 1× Tris-buffered saline (TBS)–Tween 20 (0.05%) (TBST) three times for 5 min each time. Duolink anti-rabbit plus and anti-mouse minus *in situ* proximity ligation assay (PLA) probes were added to the samples (1:5 dilution) and incubated at 37°C for 1 h. After the incubation step, washes were done with 1× TBST twice for 5 min each time. The ligation stock was diluted 1:5 in high-purity water and added to the wells (40 μl), and the slides were incubated at 37°C for 30 min. The slides were washed with buffer A (Duolink II kit; Sigma-Aldrich, Inc.) three times for 5 min each time, amplification solution (40 μl) was added, and the slides were incubated for 1.5 h at 37°C. Subsequently, the slides were washed with wash buffer B twice for 10 min each time and once with 0.01% buffer B (Duolink II kit). The slides were mounted with mounting medium (Duolink II), stored at −20°C, and protected from light until confocal images were taken. The confocal images were taken using a 60× objective on an Olympus Fluoview FV10i confocal laser scanning microscope.

Immunoprecipitation and immunoblot assays. SK-N-SH cells were infected with the McKrae wild-type and McKrae gKΔ31-68 viruses at an MOI of 10. At 1 hpi, the infected cells were lysed with NP-40 cell lysis buffer (Life Technologies) supplemented with protease inhibitor tablets (Roche). The samples were centrifuged at 13,000 rpm for 10 min at 4°C. Subsequently, the supernatants were used for immunoprecipitation. The proteins from virus-infected cells were immunoprecipitated using protein G magnetic Dynabeads according to the manufacturer's instructions (Invitrogen). Briefly, the beads were bound to their respective antibodies and left on a nutator for 10 min, followed by the addition of cell lysates. The lysate-bead mixture was kept on the nutator for 10 min at room temperature and subsequently washed three times with phosphate-buffered saline (PBS). The protein was eluted from the magnetic beads in 40 μl of elution buffer and used for immunoblot assays. Sample buffer containing 5% β-mercaptoethanol was added to the protein, and the mixture was heated at 55°C for 15 min. Proteins were resolved in a 4 to 20% SDS-PAGE gel and immobilized on nitrocellulose membranes. For Western immunoblot assays, subconfluent SK-N-SH cells were infected with the indicated viruses at an MOI of 10 for different times, as mentioned elsewhere in the article. The cells were lysed with NP-40 lysis buffer, and the lysate was used for Western immunoblot assays. Immunoblot assays were carried out using monoclonal mouse anti-gB antibody (Abcam), rabbit anti-Akt-1(S473) antibody (Millipore), horseradish peroxidase (HRP)-conjugated goat anti-mouse immunoglobulin antibodies against the light chain (Fab) and heavy chain (Fc) (Abcam, Inc., Cambridge, MA), and HRP-conjugated goat anti-rabbit immunoglobulin antibody (Abcam, Inc., Cambridge, MA).

Calcium signaling assay. Vero and neuroblastoma (SK-N-SH) cells were grown in 96-well black clear-bottom plates overnight. The cells were washed twice with PBS and incubated with a calcium indicator (Fura-2AM) dye solution (25 μM) at 37°C for 30 min. The cells were washed twice with PBS and kept on ice for 5 min. The cells were infected with purified viruses at an MOI of 10 in PBS, while PBS alone was added to mock-infected cells, and the cells were incubated at 4°C for an hour for adsorption. Then, the fluorescence was measured every minute for an hour by use of a SpectraMax M2 microplate reader, which was set at 37°C. The excitation and emission wavelengths for Fura-2AM were 340/380 nm and 510 nm, respectively, and the intracellular calcium concentration was measured by calculation of the ratio of bound to unbound dye following the equation mentioned elsewhere (77). The individual calcium concentrations (60 time points) over the 1-h time period were used to produce an overall average value of intracellular calcium concentration.

PS detection on cell surface. Vero cells were grown on 8-well chamber slides, adsorbed with both the McKrae and McKrae gKΔ31-68 viruses at an MOI of 10 at 4°C for 1 h, and shifted to a temperature of 37°C for 5 min. Then, the cells were washed twice with 1× PBS and once with 1× annexin binding buffer. Then, the cells were stained with FITC-annexin V for 5 min at room temperature. After this, images were immediately taken. A 40× objective lens was used. Six different areas of 480 mm^2 each were randomly chosen from each well, and then the green signal was counted. Each sample was tested in triplicate. Each value was converted to 100 mm^2, and the average value was taken for making the graph.

Akt-1(S473) detection on the cell surface. Vero cells were grown on 8-well chamber slides and infected with both the McKrae VP26-EGFP and gKΔ31-68 VP26-EGFP viruses at an MOI of 10 at 37°C, and after 30 min, rabbit anti Akt-1(S473) antibody (1:100) was added under live conditions and the mixture was incubated for 30 min at 37°C. Subsequently, the cells were washed with 1× PBS, fixed with formalin, and reacted with goat anti-rabbit IgG conjugated with Alexa Fluor 594 (red) for 1 h at 37°C. Cell mask deep red plasma membrane stain was added to the cells (8 μg/ml), and the cells were incubated at 37°C for a minute and washed with 1× PBS. The slides were then mounted with DAPI (4′,6-diamidino-2-phenylindole) containing mounting medium and observed under a confocal microscope at a magnification of 63× with oil immersion. Uninfected cells were stained for the intracellular protein dynein as a negative control in the same way described above (with mouse antidynein antibody under live conditions and then fixed). Infected cells were permeabilized with methanol, reacted with rabbit anti-Akt-1(S473) and goat anti-rabbit IgG conjugated with Alexa Fluor 594, and mounted in the same way

described above with DAPI to show the intracellular Akt-1(S473). Uninfected cells were permeabilized and stained for the intracellular protein dynein in the same way described above to show cytoplasmic dynein.

Endocytosis inhibition assay. To assess the inhibition of endocytosis, two inhibitors were used. Pitstop-2 is a clathrin inhibitor, and dynasore hydrate is a dynamin inhibitor. SK-N-SH cells were treated with the drugs for 30 min at 37°C. The drugs were used with either 30 μM pitstop-2 or 80 μM dynasore hydrate alone and with 30 μM pitstop-2 plus 80 μM dynasore hydrate in combination. The cells were then infected with the McKrae and McKrae gKΔ31-68 viruses at an MOI of 10 for 1 h at 37°C with the drugs. In the case of Vero cells, a series of dilutions of pitstop-2 in combination with dynasore hydrate (80 μM) was added, and then the cells were infected with the McKrae and McKrae gKΔ31-68 viruses at 100 PFU for 48 h at 37°C and the plaques were counted.

Statistical analyses. Statistical analyses were performed by using analysis of variance (ANOVA) and Student's *t* tests; values of P of <0.05 were considered significant. Bonferroni adjustments were applied for multiple comparisons between each treatment group and the control. All analyses were performed using GraphPad Prism (version 5) software (GraphPad Software, San Diego, CA, USA).

ACKNOWLEDGMENTS

The work was supported by the LSU Division of Biotechnology & Molecular Medicine, by a Governor's Biotechnology Initiative grant (to K.G.K.), and by Cores of the Center for Experimental Infectious Disease Research (CEIDR), funded by NIH, NIGMS, grant P30GM110670.

We thank Tarlan Mokhtarzadeh for graphical assistance with Fig. 7.

REFERENCES

1. Roizman B, Knipe DM. 2001. Herpes simplex viruses and their replication, p 2399–2459. *In* Knipe DM, Howley PM, Chanock RM, Melnick JL, Monath TP, Roizman B, Straus SE (ed), Fields virology, 3rd ed, vol 2. Lippincott-Williams & Wilkins, Philadelphia, PA.
2. Aggarwal A, Miranda-Saksena M, Boadle RA, Kelly BJ, Diefenbach RJ, Alam W, Cunningham AL. 2012. Ultrastructural visualization of individual tegument protein dissociation during entry of herpes simplex virus 1 into human and rat dorsal root ganglion neurons. J Virol 86:6123–6137. https://doi.org/10.1128/JVI.07016-11.
3. Nicola AV. 2016. Herpesvirus entry into host cells mediated by endosomal low pH. Traffic 17:965–975. https://doi.org/10.1111/tra.12408.
4. Eisenberg RJ, Atanasiu D, Cairns TM, Gallagher JR, Krummenacher C, Cohen GH. 2012. Herpes virus fusion and entry: a story with many characters. Viruses 4:800–832. https://doi.org/10.3390/v4050800.
5. Lycke E, Hamark B, Johansson M, Krotochwil A, Lycke J, Svennerholm B. 1988. Herpes simplex virus infection of the human sensory neuron. An electron microscopy study. Arch Virol 101:87–104.
6. Nicola AV, Hou J, Major EO, Straus SE. 2005. Herpes simplex virus type 1 enters human epidermal keratinocytes, but not neurons, via a pH-dependent endocytic pathway. J Virol 79:7609–7616. https://doi.org/10.1128/JVI.79.12.7609-7616.2005.
7. Maurer UE, Sodeik B, Grunewald K. 2008. Native 3D intermediates of membrane fusion in herpes simplex virus 1 entry. Proc Natl Acad Sci U S A 105:10559–10564. https://doi.org/10.1073/pnas.0801674105.
8. Rahn E, Petermann P, Hsu MJ, Rixon FJ, Knebel-Morsdorf D. 2011. Entry pathways of herpes simplex virus type 1 into human keratinocytes are dynamin- and cholesterol-dependent. PLoS One 6:e25464. https://doi.org/10.1371/journal.pone.0025464.
9. de Duve C. 1983. Lysosomes revisited. Eur J Biochem 137:391–397. https://doi.org/10.1111/j.1432-1033.1983.tb07841.x.
10. Nicola AV, McEvoy AM, Straus SE. 2003. Roles for endocytosis and low pH in herpes simplex virus entry into HeLa and Chinese hamster ovary cells. J Virol 77:5324–5332. https://doi.org/10.1128/JVI.77.9.5324-5332.2003.
11. Milne RS, Nicola AV, Whitbeck JC, Eisenberg RJ, Cohen GH. 2005. Glycoprotein D receptor-dependent, low-pH-independent endocytic entry of herpes simplex virus type 1. J Virol 79:6655–6663. https://doi.org/10.1128/JVI.79.11.6655-6663.2005.
12. Koyama AH, Uchida T. 1987. The mode of entry of herpes simplex virus type 1 into Vero cells. Microbiol Immunol 31:123–130. https://doi.org/10.1111/j.1348-0421.1987.tb03075.x.
13. Smith GA, Pomeranz L, Gross SP, Enquist LW. 2004. Local modulation of plus-end transport targets herpesvirus entry and egress in sensory axons. Proc Natl Acad Sci U S A 101:16034–16039. https://doi.org/10.1073/pnas.0404686101.
14. Wittels M, Spear PG. 1991. Penetration of cells by herpes simplex virus does not require a low pH-dependent endocytic pathway. Virus Res 18:271–290. https://doi.org/10.1016/0168-1702(91)90024-P.
15. Herold BC, WuDunn D, Soltys N, Spear PG. 1991. Glycoprotein C of herpes simplex virus type 1 plays a principal role in the adsorption of virus to cells and in infectivity. J Virol 65:1090–1098.
16. Shukla D, Spear PG. 2001. Herpesviruses and heparan sulfate: an intimate relationship in aid of viral entry. J Clin Invest 108:503–510. https://doi.org/10.1172/JCI200113799.
17. Geraghty RJ, Krummenacher C, Cohen GH, Eisenberg RJ, Spear PG. 1998. Entry of alphaherpesviruses mediated by poliovirus receptor-related protein 1 and poliovirus receptor. Science 280:1618–1620. https://doi.org/10.1126/science.280.5369.1618.
18. Montgomery RI, Warner MS, Lum BJ, Spear PG. 1996. Herpes simplex virus-1 entry into cells mediated by a novel member of the TNF/NGF receptor family. Cell 87:427–436. https://doi.org/10.1016/S0092-8674(00)81363-X.
19. Shukla D, Liu J, Blaiklock P, Shworak NW, Bai X, Esko JD, Cohen GH, Eisenberg RJ, Rosenberg RD, Spear PG. 1999. A novel role for 3-O-sulfated heparan sulfate in herpes simplex virus 1 entry. Cell 99:13–22. https://doi.org/10.1016/S0092-8674(00)80058-6.
20. Satoh T, Arii J, Suenaga T, Wang J, Kogure A, Uehori J, Arase N, Shiratori I, Tanaka S, Kawaguchi Y, Spear PG, Lanier LL, Arase H. 2008. PILRalpha is a herpes simplex virus-1 entry coreceptor that associates with glycoprotein B. Cell 132:935–944. https://doi.org/10.1016/j.cell.2008.01.043.
21. Arii J, Goto H, Suenaga T, Oyama M, Kozuka-Hata H, Imai T, Minowa A, Akashi H, Arase H, Kawaoka Y, Kawaguchi Y. 2010. Non-muscle myosin IIA is a functional entry receptor for herpes simplex virus-1. Nature 467:859–862. https://doi.org/10.1038/nature09420.
22. Suenaga T, Satoh T, Somboonthum P, Kawaguchi Y, Mori Y, Arase H. 2010. Myelin-associated glycoprotein mediates membrane fusion and entry of neurotropic herpesviruses. Proc Natl Acad Sci U S A 107:866–871. https://doi.org/10.1073/pnas.0913351107.
23. Chowdhury S, Chouljenko VN, Naderi M, Kousoulas KG. 2013. The amino terminus of herpes simplex virus 1 glycoprotein K is required for virion entry via the paired immunoglobulin-like type-2 receptor alpha. J Virol 87:3305–3313. https://doi.org/10.1128/JVI.02982-12.
24. Cai WH, Gu B, Person S. 1988. Role of glycoprotein B of herpes simplex virus type 1 in viral entry and cell fusion. J Virol 62:2596–2604.
25. Desai PJ, Schaffer PA, Minson AC. 1988. Excretion of non-infectious virus particles lacking glycoprotein H by a temperature-sensitive mutant of herpes simplex virus type 1: evidence that gH is essential for virion infectivity. J Gen Virol 69:1147. https://doi.org/10.1099/0022-1317-69-6-1147.
26. Hutchinson L, Browne H, Wargent V, Davis-Poynter N, Primorac S, Goldsmith K, Minson AC, Johnson DC. 1992. A novel herpes simplex virus

glycoprotein, gL, forms a complex with glycoprotein H (gH) and affects normal folding and surface expression of gH. J Virol 66:2240–2250.
27. Ligas MW, Johnson DC. 1988. A herpes simplex virus mutant in which glycoprotein D sequences are replaced by beta-galactosidase sequences binds to but is unable to penetrate into cells. J Virol 62:1486–1494.
28. Campadelli-Fiume G, Menotti L, Avitabile E, Gianni T. 2012. Viral and cellular contributions to herpes simplex virus entry into the cell. Curr Opin Virol 2:28–36. https://doi.org/10.1016/j.coviro.2011.12.001.
29. Connolly SA, Jackson JO, Jardetzky TS, Longnecker R. 2011. Fusing structure and function: a structural view of the herpesvirus entry machinery. Nat Rev Microbiol 9:369–381. https://doi.org/10.1038/nrmicro2548.
30. Pertel PE, Fridberg A, Parish ML, Spear PG. 2001. Cell fusion induced by herpes simplex virus glycoproteins gB, gD, and gH-gL requires a gD receptor but not necessarily heparan sulfate. Virology 279:313–324. https://doi.org/10.1006/viro.2000.0713.
31. Terry-Allison T, Montgomery RI, Warner MS, Geraghty RJ, Spear PG. 2001. Contributions of gD receptors and glycosaminoglycan sulfation to cell fusion mediated by herpes simplex virus 1. Virus Res 74:39–45. https://doi.org/10.1016/S0168-1702(00)00244-6.
32. Terry-Allison T, Montgomery RI, Whitbeck JC, Xu R, Cohen GH, Eisenberg RJ, Spear PG. 1998. HveA (herpesvirus entry mediator A), a coreceptor for herpes simplex virus entry, also participates in virus-induced cell fusion. J Virol 72:5802–5810.
33. Atanasiu D, Saw WT, Cohen GH, Eisenberg RJ. 2010. Cascade of events governing cell-cell fusion induced by herpes simplex virus glycoproteins gD, gH/gL, and gB. J Virol 84:12292–12299. https://doi.org/10.1128/JVI.01700-10.
34. Davis-Poynter N, Bell S, Minson T, Browne H. 1994. Analysis of the contributions of herpes simplex virus type 1 membrane proteins to the induction of cell-cell fusion. J Virol 68:7586–7590.
35. Visalli RJ, Brandt CR. 1991. The HSV-1 UL45 gene product is not required for growth in Vero cells. Virology 185:419–423. https://doi.org/10.1016/0042-6822(91)90790-I.
36. Haanes EJ, Nelson CM, Soule CL, Goodman JL. 1994. The UL45 gene product is required for herpes simplex virus type 1 glycoprotein B-induced fusion. J Virol 68:5825–5834.
37. Foster TP, Melancon JM, Baines JD, Kousoulas KG. 2004. The herpes simplex virus type 1 UL20 protein modulates membrane fusion events during cytoplasmic virion morphogenesis and virus-induced cell fusion. J Virol 78:5347–5357. https://doi.org/10.1128/JVI.78.10.5347-5357.2004.
38. Melancon JM, Fulmer PA, Kousoulas KG. 2007. The herpes simplex virus UL20 protein functions in glycoprotein K (gK) intracellular transport and virus-induced cell fusion are independent of UL20 functions in cytoplasmic virion envelopment. Virol J 4:120. https://doi.org/10.1186/1743-422X-4-120.
39. Chouljenko VN, Iyer AV, Chowdhury S, Chouljenko DV, Kousoulas KG. 2009. The amino terminus of herpes simplex virus type 1 glycoprotein K (gK) modulates gB-mediated virus-induced cell fusion and virion egress. J Virol 83:12301–12313. https://doi.org/10.1128/JVI.01329-09.
40. Debroy C, Pederson N, Person S. 1985. Nucleotide sequence of a herpes simplex virus type 1 gene that causes cell fusion. Virology 145:36–48. https://doi.org/10.1016/0042-6822(85)90199-0.
41. MacLean CA, Efstathiou S, Elliott ML, Jamieson FE, McGeoch DJ. 1991. Investigation of herpes simplex virus type 1 genes encoding multiply inserted membrane proteins. J Gen Virol 72(Pt 4):897–906. https://doi.org/10.1099/0022-1317-72-4-897.
42. Ramaswamy R, Holland TC. 1992. In vitro characterization of the HSV-1 UL53 gene product. Virology 186:579–587. https://doi.org/10.1016/0042-6822(92)90024-J.
43. Foster TP, Alvarez X, Kousoulas KG. 2003. Plasma membrane topology of syncytial domains of herpes simplex virus type 1 glycoprotein K (gK): the UL20 protein enables cell surface localization of gK but not gK-mediated cell-to-cell fusion. J Virol 77:499–510. https://doi.org/10.1128/JVI.77.1.499-510.2003.
44. Melancon JM, Foster TP, Kousoulas KG. 2004. Genetic analysis of the herpes simplex virus type 1 (HSV-1) UL20 protein domains involved in cytoplasmic virion envelopment and virus-induced cell fusion. J Virol 78:7329–7343. https://doi.org/10.1128/JVI.78.14.7329-7343.2004.
45. Dietz P, Klupp BG, Fuchs W, Kollner B, Weiland E, Mettenleiter TC. 2000. Pseudorabies virus glycoprotein K requires the UL20 gene product for processing. J Virol 74:5083–5090. https://doi.org/10.1128/JVI.74.11.5083-5090.2000.
46. Fuchs W, Klupp BG, Granzow H, Mettenleiter TC. 1997. The UL20 gene product of pseudorabies virus functions in virus egress. J Virol 71:5639–5646.
47. Foster TP, Chouljenko VN, Kousoulas KG. 2008. Functional and physical interactions of the herpes simplex virus type 1 UL20 membrane protein with glycoprotein K. J Virol 82:6310–6323. https://doi.org/10.1128/JVI.00147-08.
48. Foster TP, Melancon JM, Kousoulas KG. 2001. An alpha-helical domain within the carboxyl terminus of herpes simplex virus type 1 (HSV-1) glycoprotein B (gB) is associated with cell fusion and resistance to heparin inhibition of cell fusion. Virology 287:18–29. https://doi.org/10.1006/viro.2001.1004.
49. Foster TP, Melancon JM, Olivier TL, Kousoulas KG. 2004. Herpes simplex virus type 1 glycoprotein K and the UL20 protein are interdependent for intracellular trafficking and trans-Golgi network localization. J Virol 78:13262–13277. https://doi.org/10.1128/JVI.78.23.13262-13277.2004.
50. Jambunathan N, Chowdhury S, Subramanian R, Chouljenko VN, Walker JD, Kousoulas KG. 2011. Site-specific proteolytic cleavage of the amino terminus of herpes simplex virus glycoprotein K on virion particles inhibits virus entry. J Virol 85:12910–12918. https://doi.org/10.1128/JVI.06268-11.
51. Foster TP, Kousoulas KG. 1999. Genetic analysis of the role of herpes simplex virus type 1 glycoprotein K in infectious virus production and egress. J Virol 73:8457–8468.
52. Hutchinson L, Roop-Beauchamp C, Johnson DC. 1995. Herpes simplex virus glycoprotein K is known to influence fusion of infected cells, yet is not on the cell surface. J Virol 69:4556–4563.
53. Jayachandra S, Baghian A, Kousoulas KG. 1997. Herpes simplex virus type 1 glycoprotein K is not essential for infectious virus production in actively replicating cells but is required for efficient envelopment and translocation of infectious virions from the cytoplasm to the extracellular space. J Virol 71:5012–5024.
54. Chouljenko VN, Iyer AV, Chowdhury S, Kim J, Kousoulas KG. 2010. The herpes simplex virus type 1 UL20 protein and the amino terminus of glycoprotein K (gK) physically interact with gB. J Virol 84:8596–8606. https://doi.org/10.1128/JVI.00298-10.
55. Foster TP, Rybachuk GV, Kousoulas KG. 2001. Glycoprotein K specified by herpes simplex virus type 1 is expressed on virions as a Golgi complex-dependent glycosylated species and functions in virion entry. J Virol 75:12431–12438. https://doi.org/10.1128/JVI.75.24.12431-12438.2001.
56. Rider PJF, Naderi M, Bergeron S, Chouljenko VN, Brylinski M, Kousoulas KG. 2017. Cysteines and N-glycosylation sites conserved among all alphaherpesviruses regulate membrane fusion in herpes simplex virus type 1 infection. J Virol 91:e00873-17. https://doi.org/10.1128/JVI.00873-17.
57. David AT, Baghian A, Foster TP, Chouljenko VN, Kousoulas KG. 2008. The herpes simplex virus type 1 (HSV-1) glycoprotein K (gK) is essential for viral corneal spread and neuroinvasiveness. Curr Eye Res 33:455–467. https://doi.org/10.1080/02713680802130362.
58. David AT, Saied A, Charles A, Subramanian R, Chouljenko VN, Kousoulas KG. 2012. A herpes simplex virus 1 (McKrae) mutant lacking the glycoprotein K gene is unable to infect via neuronal axons and egress from neuronal cell bodies. mBio 3:e00144-12. https://doi.org/10.1128/mBio.00144-12.
59. Saied AA, Chouljenko VN, Subramanian R, Kousoulas KG. 2014. A replication competent HSV-1(McKrae) with a mutation in the amino-terminus of glycoprotein K (gK) is unable to infect mouse trigeminal ganglia after cornea infection. Curr Eye Res 39:596–603. https://doi.org/10.3109/02713683.2013.855238.
60. Hemmings BA, Restuccia DF. 2012. PI3K-PKB/Akt pathway. Cold Spring Harb Perspect Biol 4:a011189. https://doi.org/10.1101/cshperspect.a011189.
61. Brodbeck D, Cron P, Hemmings BA. 1999. A human protein kinase Bgamma with regulatory phosphorylation sites in the activation loop and in the C-terminal hydrophobic domain. J Biol Chem 274:9133–9136. https://doi.org/10.1074/jbc.274.14.9133.
62. Cheng JQ, Godwin AK, Bellacosa A, Taguchi T, Franke TF, Hamiliton TC, Tsichlis PN, Testa JR. 1992. Akt2, a putative oncogene encoding a member of a subfamily of protein-serine/threonine kinase, is amplified in human ovarian carcinomas. Proc Natl Acad Sci U S A 89:9267–9271. https://doi.org/10.1073/pnas.89.19.9267.
63. Jones PF, Jakubowiczt T, Hemmings BA. 1991. Molecular cloning of a second form of rac protein kinase. Cell Regul 2:1001–1009.
64. Jones PF, Jakubowiczt T, Pitossi FJ, Maurer F, Hemmings BA. 1991. Molecular cloning and identification of a serine/threonine protein kinase

of the second-messenger subfamily. Proc Natl Acad Sci U S A 88:4171–4175. https://doi.org/10.1073/pnas.88.10.4171.
65. Masure S, Haefner B, Wesselink JJ, Hoefnagel E, Mortier E, Verhasselt P, Tuytelaars A, Gordon R, Richardson A. 1999. Molecular cloning, expression and characterization of the human serine/threonine kinase Akt-3. Eur J Biochem 265:353–360. https://doi.org/10.1046/j.1432-1327.1999.00774.x.
66. Nakatani K, Thompson DA, Barthel A, Sakaue H, Liu W, Weigel RJ, Roth RA. 1999. Up-regulation of Akt3 in estrogen receptor-deficient breast cancer and androgen-independent prostate cancer lines. J Biol Chem 274:21528–21532. https://doi.org/10.1074/jbc.274.31.21528.
67. Hers I, Vincent EE, Tavare JM. 2011. Akt signalling in health and disease. Cell Signal 23:1515–1527. https://doi.org/10.1016/j.cellsig.2011.05.004.
68. Brazil DP, Hemmings BA. 2001. Ten years of protein kinase B signalling: a hard Akt to follow. Trends Biochem 26:657–664. https://doi.org/10.1016/S0968-0004(01)01958-2.
69. Chan TO, Rittenhouse SE, Tsichlis PN. 1999. AKT/PKB and other D3 phosphoinositide-regulated kinases: kinase activation by phosphoinositide-dependent phosphorylation. Annu Rev Biochem 68:965–1014. https://doi.org/10.1146/annurev.biochem.68.1.965.
70. Downward J. 1998. Lipid-regulated kinases: some common themes at last. Science 279:673–674. https://doi.org/10.1126/science.279.5351.673.
71. Hemmings BA. 1997. Akt signaling: linking membrane events to life and death decisions. Science 275:628–630. https://doi.org/10.1126/science.275.5300.628.
72. Kandel ES, Hay N. 1999. The regulation and activities of the multifunctional serine/threonine kinase Akt/PKB. Exp Cell Res 253:210–229. https://doi.org/10.1006/excr.1999.4690.
73. Scheid MP, Woodgett JR. 2001. PKB/AKT: functional insights from genetic models. Nat Rev Mol Cell Biol 2:760–768.
74. Norman KL, Sarnow P. 2010. Herpes simplex virus is Akt-ing in translational control. Genes Dev 24:2583–2586. https://doi.org/10.1101/gad.2004510.
75. Liu X, Cohen JI. 2015. The role of PI3K/Akt in human herpesvirus infection: from the bench to the bedside. Virology 479-480:568–577. https://doi.org/10.1016/j.virol.2015.02.040.
76. MacLeod IJ, Minson T. 2010. Binding of herpes simplex virus type-1 virions leads to the induction of intracellular signalling in the absence of virus entry. PLoS One 5:e9560. https://doi.org/10.1371/journal.pone.0009560.
77. Cheshenko N, Trepanier JB, Stefanidou M, Buckley N, Gonzalez P, Jacobs W, Herold BC. 2013. HSV activates Akt to trigger calcium release and promote viral entry: novel candidate target for treatment and suppression. FASEB J 27:2584–2599. https://doi.org/10.1096/fj.12-220285.
78. Cheshenko N, Del Rosario B, Woda C, Marcellino D, Satlin LM, Herold BC. 2003. Herpes simplex virus triggers activation of calcium-signaling pathways. J Cell Biol 163:283–293. https://doi.org/10.1083/jcb.200301084.
79. Azab W, Gramatica A, Herrmann A, Osterrieder N. 2015. Binding of alphaherpesvirus glycoprotein H to surface alpha4beta1-integrins activates calcium-signaling pathways and induces phosphatidylserine exposure on the plasma membrane. mBio 6:e01552-15. https://doi.org/10.1128/mBio.01552-15.
80. Chugh P, Bradel-Tretheway B, Monteiro-Filho CM, Planelles V, Maggirwar SB, Dewhurst S, Kim B. 2008. Akt inhibitors as an HIV-1 infected macrophage-specific anti-viral therapy. Retrovirology 5:11. https://doi.org/10.1186/1742-4690-5-11.
81. Jambunathan N, Charles AS, Subramanian R, Saied AA, Naderi M, Rider P, Brylinski M, Chouljenko VN, Kousoulas KG. 2015. Deletion of a predicted beta-sheet domain within the amino terminus of herpes simplex virus glycoprotein K conserved among alphaherpesviruses prevents virus entry into neuronal axons. J Virol 90:2230–2239. https://doi.org/10.1128/JVI.02468-15.
82. Person S, Kousoulas KG, Knowles RW, Read GS, Holland TC, Keller PM, Warner SC. 1982. Glycoprotein processing in mutants of HSV-1 that induce cell fusion. Virology 117:293–306. https://doi.org/10.1016/0042-6822(82)90470-6.
83. Berridge MJ. 2005. Unlocking the secrets of cell signaling. Annu Rev Physiol 67:1–21. https://doi.org/10.1146/annurev.physiol.67.040103.152647.
84. Cheshenko N, Liu W, Satlin LM, Herold BC. 2007. Multiple receptor interactions trigger release of membrane and intracellular calcium stores critical for herpes simplex virus entry. Mol Biol Cell 18:3119–3130. https://doi.org/10.1091/mbc.E07-01-0062.
85. Frasch SC, Henson PM, Nagaosa K, Fessler MB, Borregaard N, Bratton DL. 2004. Phospholipid flip-flop and phospholipid scramblase 1 (PLSCR1) co-localize to uropod rafts in formylated Met-Leu-Phe-stimulated neutrophils. J Biol Chem 279:17625–17633. https://doi.org/10.1074/jbc.M313414200.
86. Dutta D, Williamson CD, Cole NB, Donaldson JG. 2012. Pitstop 2 is a potent inhibitor of clathrin-independent endocytosis. PLoS One 7:e45799. https://doi.org/10.1371/journal.pone.0045799.
87. Macia E, Ehrlich M, Massol R, Boucrot E, Brunner C, Kirchhausen T. 2006. Dynasore, a cell-permeable inhibitor of dynamin. Dev Cell 10:839–850. https://doi.org/10.1016/j.devcel.2006.04.002.
88. Bond VC, Person S. 1984. Fine structure physical map locations of alterations that affect cell fusion in herpes simplex virus type 1. Virology 132:368–376. https://doi.org/10.1016/0042-6822(84)90042-4.
89. Pogue-Geile KL, Lee GT, Shapira SK, Spear PG. 1984. Fine mapping of mutations in the fusion-inducing MP strain of herpes simplex virus type 1. Virology 136:100–109. https://doi.org/10.1016/0042-6822(84)90251-4.
90. Ruyechan WT, Morse LS, Knipe DM, Roizman B. 1979. Molecular genetics of herpes simplex virus. II. Mapping of the major viral glycoproteins and of the genetic loci specifying the social behavior of infected cells. J Virol 29:677–697.
91. Holm CK, Jensen SB, Jakobsen MR, Cheshenko N, Horan KA, Moeller HB, Gonzalez-Dosal R, Rasmussen SB, Christensen MH, Yarovinsky TO, Rixon FJ, Herold BC, Fitzgerald KA, Paludan SR. 2012. Virus-cell fusion as a trigger of innate immunity dependent on the adaptor STING. Nat Immunol 13:737–743. https://doi.org/10.1038/ni.2350.
92. Hare DN, Collins SE, Mukherjee S, Loo YM, Gale M, Jr, Janssen LJ, Mossman KL. 2015. Membrane perturbation-associated Ca^{2+} signaling and incoming genome sensing are required for the host response to low-level enveloped virus particle entry. J Virol 90:3018–3027. https://doi.org/10.1128/JVI.02642-15.
93. Osterrieder K. 2017. Cell biology of herpes viruses. Springer, Berlin, Germany.
94. Stanfield BA, Stahl J, Chouljenko VN, Subramanian R, Charles AS, Saied AA, Walker JD, Kousoulas KG. 2014. A single intramuscular vaccination of mice with the HSV-1 VC2 virus with mutations in the glycoprotein K and the membrane protein UL20 confers full protection against lethal intravaginal challenge with virulent HSV-1 and HSV-2 strains. PLoS One 9:e109890. https://doi.org/10.1371/journal.pone.0109890.
95. Stanfield BA, Pahar B, Chouljenko VN, Veazey R, Kousoulas KG. 2017. Vaccination of rhesus macaques with the live-attenuated HSV-1 vaccine VC2 stimulates the proliferation of mucosal T cells and germinal center responses resulting in sustained production of highly neutralizing antibodies. Vaccine 35:536–543. https://doi.org/10.1016/j.vaccine.2016.12.018.
96. Jambunathan N, Chouljenko D, Desai P, Charles AS, Subramanian R, Chouljenko VN, Kousoulas KG. 2014. Herpes simplex virus 1 protein UL37 interacts with viral glycoprotein gK and membrane protein UL20 and functions in cytoplasmic virion envelopment. J Virol 88:5927–5935. https://doi.org/10.1128/JVI.00278-14.